Biofuel Research Journal 38 (2023) 1816-1829

Biofuel Research Journal

Journal homepage: www.biofueljournal.com

Original Research Paper

Thermodynamic method for analyzing and optimizing pretreatment/anaerobic digestion systems

Lee D. Hansen[1,2,*]

[1] *Department of Chemistry and Biochemistry, Brigham Young University, Provo, UT 84602, USA.*

[2] *Verde Technologies, Springville, UT, USA.*

HIGHLIGHTS

- Dairy manure digestion with pre-digestion with *Caldicellulosiruptor bescii* is modeled with thermodynamics.
- Syntrophic methanogenesis is inhibited by acetate.
- Acetoclastic methanogenesis is accelerated by increasing acetate.
- Acetoclastic methanogenesis is ≈1.4 times faster than syntrophic methanogenesis.
- The correct ratio of acetoclastic and syntrophic methanogenesis maximizes biogas.

GRAPHICAL ABSTRACT

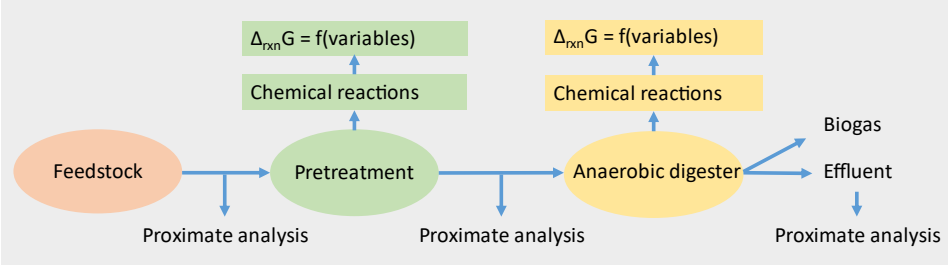

ARTICLE INFO

Article history:
Received 4 March 2023
Received in revised form 7 April 2023
Accepted 10 May 2023
Published 1 June 2023

Keywords:
Acetoclastic
Syntrophic
Methanogenesis
Acetate
Volatile fatty acids
Caldicellulosiruptor bescii

ABSTRACT

This paper builds a quantitative thermodynamic model for the microbial hydrolysis process (MHP, which uses *Caldicellulosiruptor bescii* at 75°C for pre-digestion) for producing biogas from a 5-10% aqueous suspension of dairy manure (naturally buffered near pH 7.8 by ammonium bicarbonate) by anaerobic digestion with a mix of acetoclastic and syntrophic methanogenesis. Standard Gibbs energy changes were calculated for the major reactions in pre-digestion, for reactions producing H_2, acetate, and CO_2 in the digester, and for methanogenesis reactions in the digester. The available data limit the study to analyzing reactions in the digester to reactions of short-chain volatile fatty acids anions. Results are presented as curves of $\Delta_{rxn}G$ (Gibbs energy change) *vs.* acetate concentration. The H_2(aq) concentration must be above 1.2×10^{-9} M to get significant syntrophic methanogenesis, i.e., for $\Delta_{rxn}G$ to be negative. The results show syntrophic methanogenesis of propionate, butyrate, and valerate slows as acetate concentration increases because hydrogen production also decreases, and consequently, biogas production from syntrophic methanogenesis slows as acetate increases. Bicarbonate also inhibits both acetoclastic and syntrophic methanogenesis but is necessary to prevent acidification (souring) of the digester. At identical steady-state conditions, acetoclastic methanogenesis runs about 1.4 times faster than syntrophic methanogenesis. Because syntrophic methanogenesis produces acetate catabolized by acetoclastic methanogens, both types of methanogens are necessary to maximize biogas production. The culture in the digester is predicted to evolve to optimize the ratio of acetoclastic methanogens to syntrophic methanogens, a condition signaled by a constant, low acetate concentration in the digester effluent. Obtaining volatile solids reduction as high as 75% with MHP requires a feedstock with less than 25% lignin and a culture of acetoclastic methanogens and syntrophic methanogens and their symbiotic bacteria.

* Corresponding author at:
E-mail address: ldhansen@chem.byu.edu

Please cite this article as: Hansen L.D. Thermodynamic method for analyzing and optimizing pretreatment/anaerobic digestion systems. Biofuel Research Journal 38 (2023) 1816-1829. DOI: 10.18331/BRJ2023.10.2.2

Contents

Abbreviations

MHP	Microbial hydrolysis process
AD	Anaerobic digestion
VS	Volatile solids
ASB	Anaerobic secretome bioreactor
VFA	Volatile fatty acids
NA	Not available
K_M	Michaelis-Menten constant
M, mM	Mole L^{-1}, Millimole L^{-1}
$\Delta_f G°$	Gibbs energy of formation (kJ mol^{-1})
$\Delta_{rxn} G°$	Gibbs energy change for a reaction with all reactants and products in their standard state (kJ mol^{-1})
$\Delta_{rxn} G$	Gibbs energy change for a reaction with reactants and products in non-standard states (kJ mol^{-1})
$\Delta_f H°$	Enthalpy change for formation (kJ mol^{-1})
$\Delta_{rxn} H°$	Enthalpy change for a reaction with reactants and products in their standard states (kJ mol^{-1})
S°	Entropy of a compound or ion in the standard state (J mol^{-1} K^{-1})
$C_p°$	Heat capacity at constant pressure
(aq), (g), (l), (s)	Aqueous, gas, liquid, and solid phase, respectively
R	Gas constant
T	Thermodynamic temperature (K, unless °C is specified)
K_{eq}	Equilibrium constant
Q	Reaction quotient
pK_a	Negative $\log_{10}$ of the ionization constant of an acid

1. Introduction

1.1. Microbial Hydrolysis Process (MHP)

The Microbial Hydrolysis Process (MHP), developed and patented by Verde Technologies, converts organic wastes into biogas in a two-step process. The first step is the pre-digestion of a 5-10% aqueous suspension with a hyperthermophilic anaerobic bacteria, *Caldicellulosiruptor bescii*, at pH 7.8 and 75°C. The second step is anaerobic digestion (AD) with a mixed culture of hydrogen-producing bacteria, syntrophic methanogens, and acetoclastic methanogens matched to the effluent from pre-digestion. This paper specifically discusses the use of MHP for the digestion of dairy manure. Dairy manure is an organic waste available in large, concentrated, constant amounts and is an excellent material for AD. Dairy manure consists of feces and urine from cows that mainly consists of organic material (lignin, cellulose, hemicelluloses, fatty acids, urea, bacteria, and other microorganisms), significant amounts of ammonia and potassium, and trace amounts of sulfur, iron, magnesium, copper, cobalt, and manganese (Gupta et al., 2016). The composition depends somewhat on breed and food. When heated to 75°C for the pre-digestion, dairy manure creates its own ammonium bicarbonate buffer with a pH centered at 7.8 and with sufficient alkalinity for the process. Dairy manure is thus an excellent substrate for the growth of the microorganisms used in the MHP.

C. bescii makes a suite of hydrolase enzymes that partially depolymerize lignin, hydrolyze cellulose and hemicellulose into water-soluble sugars and hydrolyze esters and proteins into small, water-soluble ions and molecules. *C. bescii* catabolizes the released sugars to acetate and lactate (Kataeva et al., 2013), substrates for rapid, efficient methanogenesis by acetoclastic (also known as acetotrophic and aceticlastic) methanogens. The hydrolyzed solution/suspension is transferred to anaerobic digesters where the acetate and other small molecules are catabolized to biogas by syntrophic and acetoclastic methanogens. The process has achieved 75% destruction of the volatile solids (VS) in dairy manure and produced biogas with as high as 75% methane, as fully described by Hansen et al. (2021).

In traditional AD installations, the raw manure is fed directly into the digesters without pretreatment. The methanogens naturally present in the manure are allowed to develop in the digester. Literature on AD sometimes identifies methanogens, but the chemical composition of the feedstock is not used to optimize the consortia of microorganisms. Instead, evolution is assumed to optimize the microbiology of the feedstock. Thus, by chance, some AD installations obtain exceptional results, >40% conversion of VS into biogas, while most only get 30% or less conversion of manure VS into biogas.

The MHP changes the raw manure into a more easily digested mix of small molecules and ions. However, to optimize AD, the feedstock from MHP requires a different consortium of methanogens than traditional AD. Furthermore, MHP pasteurizes the feedstock, so the microbiology in the pre-digestion effluent/AD feed is much depleted and unsuitable for continuously seeding AD with methanogens and associated bacteria. Consequently, the digesters must be seeded at startup with a community of methanogens matched to the chemistry of the pre-digestion effluent, and retention times must be sufficient to allow for the growth of the consortium. This is both a complication and an opportunity to obtain the maximum

Please cite this article as: Hansen L.D. Thermodynamic method for analyzing and optimizing pretreatment/anaerobic digestion systems. Biofuel Research Journal 38 (2023) 1816-1829. DOI: 10.18331/BRJ2023.10.2.2

feedstock conversion into biogas in the digesters. Methanogens are exclusively archaea, obligate methane producers, and strict anaerobes. Methanogens are enormously diverse and classified into three groups based on substrate usage, hydrogenotrophic, acetoclastic, and methylotrophic (**Table 1**). Hydrogenotrophic methanogens that oxidize H_2 and reduce CO_2 to CH_4 are the most prevalent in the environment. Acetoclastic methanogens split acetate to form CH_4 and CO_2 and are found in habitats where hydrogenotrophic methanogens maintain H_2 low enough for high acetate concentrations to form (Schink, 1997; Conrad, 1999; Kato and Watanabe, 2010). Acetoclastic methanogens are the dominant methane producers in anaerobic digesters treating sewage as well as in rice fields and wetlands (Lyu et al., 2018).

Lignocellulose is the main substrate in dairy manure that is hydrolyzed by the exozymes of *C. bescii* in pre-digestion. Lignocellulose consists of bundles of cellulose bound together and protected by a sheet of lignin. The lignase exozymes produced by *C. bescii* unzip the lignin, exposing the cellulose to hydrolytic exozymes. The unzipped lignin is a dark brown-black, fibrous material much less hydrophilic than lignocellulose. The cellulase exozymes from *C. bescii* catalyze the hydrolysis of cellulose to glucose that *C. bescii* then catabolizes to produce lactate and/or acetate (Kataeva et al., 2013). Acetate is the only product from *C. bescii* catabolism found in dairy manure. Lignocellulose is not digested in traditional AD and largely accounts for the lower biogas yield.

Table 1.
The three metabolic types of methanogens, classification, and symbiotic hydrogen-producing bacteria.*

Methanogen type	Phylum/Order/Family/Genus	Symbiotic hydrogen-producing anaerobic bacteria	Ecosystem
Hydrogenotrophic	Methanopyrales, Methanococcales, and Methanobacteriales. Most Methanomicrobiales, Methanocellales, and Methanosarcinales except for Methanomassiliicoccales	*Clostridium*, *Enterobacter*, *Klebsiella*, *Citrobacter*, and *Bacillus*	Deep marine sediments, termites, human and animal guts
Acetoclastic	*Methanosarcina*, *Methanothrix*	None required	Anaerobic digesters, wetlands
Methylotrophic	Bathyarchaeota, Verstraetearchaeota, and Methanomassiliicoccales are, together with some Methanobacteriales and Methanosarcinales	None required	Marine, hypersaline, sulfate-rich

* Source: Vanwonterghem et al. (2016); Berghuis et al. (2019); Rehman et al. (2019); Conrad (2020); Westerholm et al. (2022).

Partially hydrolyzed lignin is a component in the pre-digestion effluent. **Figure 1** shows a small portion of the lignin structure and one of the major components, vanillin (Nikafshar et al., 2017). The lignin structure is held together with phenolic ester linkages hydrolyzed by the exozymes from *C. bescii* during pre-digestion. The C-C bonds are not easily broken, so the product is a fibrous material composed of partially hydrolyzed lignin. Note the $\Phi CH(OH)CH(OH)COO^-$ and $\Phi CH(OH)CH(OH)CH_2OH$ structures that are exposed by hydrolysis and may be partially digested to biogas by syntrophic methanogenesis.

Some of the compounds in the raw feedstock, i.e., volatile fatty acids (VFAs), are produced by microbes in cow guts (Mackie et al., 1991; Ahring et al., 1995; Batstone et al., 2003; Pind et al., 2003a) and are hydrolyzed by *C. bescii* exozymes from esters in the manure, but are not metabolized in pre-digestion. Except for acetate, these VFAs require syntrophic bacteria and methanogens for conversion into biogas. Consequently, optimizing AD following pre-digestion in MHP requires a mixed culture of acetoclastic methanogens, hydrogen-producing bacteria, and syntrophic methanogens. Acetate is rapidly converted to methane by acetoclastic methanogens. Syntrophic bacteria/methanogens can also metabolize acetate, but the process is much slower (Kato et al., 2014). Speciation of VFAs has been proposed as a means of determining the health of AD, and consequently, although VFAs are only a fraction (20 – 30%) of the digestible organic matter, they are the focus of this article.

1.2. Biogas production from the pre-digestion effluent

The soluble molecules and ions in the MHP that are the major contributors to biogas production are sugars from the hydrolysis of hemicellulose and cellulose, acetate from the manure and catabolism of glucose by *C. bescii*, and the anions of other VFAs; propionate, butyrate, valerate, and possibly caproate and isomers of butyrate and valerate. Complete methanogenesis of each of these compounds and ions produces the ratio of CH_4/CO_2 in the biogas, as shown in **Table 2**.

The $\%CH_4$ in biogas ranges from 50 to 100% from these reactions, depending on the mix of substrates present in the pre-digestion effluent. Note that bicarbonate is not volatile, and at pH>7, the VFAs are all non-volatile anions, so they do not create any odors. The maximum potential methane production from MHP can thus be predicted from analytical measurements of VFAs and sugars in the pre-digestion effluent, as presented in **Equation 1**.

$$N_{CH4} = 3N_{sugar} + N_{AA} + (7/4)N_{PA} + 5N_{BA} + (13/4)N_{VA} + 4N_{CA} + (3/2)N_{Lac} + xLig \quad \text{Eq. 1}$$

where N is the moles of the compound or ion per liter of ASB effluent (AA = acetate, PA = propionate, BA = n-butyrate + iso-butyrate, VA = n-valerate + iso-valerate + 2-methylbutyrate, CA = caproate + congeners, Lac = lactate, Lig = lignin). The volume of methane can be obtained from the ideal gas law at 0°C and 1 bar of methane $V_{CH4} = (22.4N_{CH4})$ = L CH_4 per L effluent, or $(0.79N_{CH4})$ = ft^3 CH_4 per L effluent.

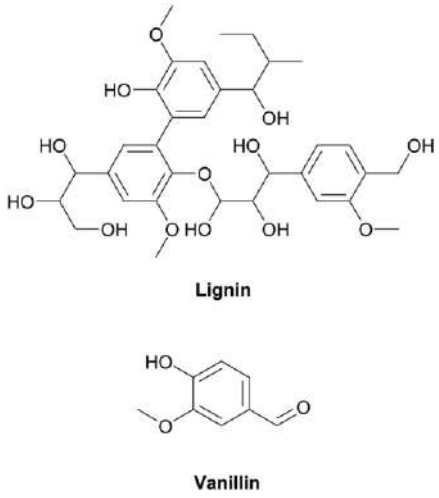

Fig. 1. The structures of lignin and vanillin, a representative monomer in the two-dimensional polymeric structure of lignin (Nikafshar et al., 2017).

1.3. Basics of the thermodynamic model for the Microbial Hydrolysis Process (MHP) using dairy manure

This paper aims to build a quantitative thermodynamic model for MHP. Such a model greatly aids in developing a quantitative understanding of the process. Obtaining accurate thermodynamic values for reactions in an

Please cite this article as: Hansen L.D. Thermodynamic method for analyzing and optimizing pretreatment/anaerobic digestion systems. Biofuel Research Journal 38 (2023) 1816-1829. DOI: 10.18331/BRJ2023.10.2.2

Table 2.
Biogas composition from the complete digestion of the small molecules and ions produced from pre-digestion in MHP

Chemical Species	Reaction	Ratio of CH_4/CO_2	$\%CH_4$
Sugars	$C_6H_{12}O_6 \rightarrow 3\ CH_4 + 3\ CO_2$	1:1	50
Lactate	$2\ CH_3CH(OH)COO^- + 2\ H_2O \rightarrow 2\ HCO_3^- + 3\ CH_4 + CO_2$	3:1	75
Caproate	$CH_3CH_2CH_2CH_2CH_2COO^- + 3\ H_2O \rightarrow HCO_3^- + 4\ CH_4 + CO_2$	4:1	80
Valerate	$4\ CH_3CH_2CH_2CH_2COO^- + 10\ H_2O \rightarrow 4\ HCO_3^- + 13\ CH_4 + 3\ CO_2$	13:3	81.3
Butyrate	$2\ CH_3CH_2CH_2COO^- + 4\ H2O \rightarrow 2\ HCO_3^- + 5\ CH_4 + CO_2$	5:1	83
Propionate	$4\ CH_3CH_2COO^- + 6\ H_2O \rightarrow 4\ HCO_3^- + 7\ CH_4 + CO_2$	7:1	87.5
Acetate	$CH_3COO^- + H_2O \rightarrow CH_4 + HCO_3^-$	1:0	100

aqueous solution requires expressing each reactant and product in the form they exist at the operating conditions in the anaerobic secretome bioreactor (ASB) and in the anaerobic digester. Pre-digestion in the ASB with *C. bescii* operates optimally at 75°C in an ammonium/bicarbonate buffer at pH 7.8. Digestion is done at a slightly lower pH at 55°C (thermophilic) or 40°C (mesophilic).

Biological chemical reactions are subject to the same thermodynamic limitations as inorganic systems. Reactions must have a negative $\Delta_{rxn}G$, i.e., a decrease in Gibbs energy before the reaction can happen to any significant extent. The necessary thermodynamic values for this project are tabulated in the literature as standard Gibbs energy changes for the formation of a compound or ion from the elements in their standard states $\Delta_fG°$. $\Delta_fG°$ values can be combined according to Hess' law to give values for the standard Gibbs energies for reactions, $\Delta_{rxn}G°$. The superscript ° indicates standard conditions, i.e., aqueous solute species at a unit activity (≈1 mole L^{-1}), gases at unit pressure (≈1 bar), and liquid water are assumed to have unit activity. $\Delta_{rxn}G°$ values are tabulated almost entirely at 25°C but can be corrected to other temperatures if enthalpy changes, $\Delta_{rxn}H°$, and thence entropy changes, $\Delta_{rxn}S°$, are also available.

The equilibrium constant, K_{eq}, for a reaction, is related to $\Delta_{rxn}G°$ by the relation (**Eq. 2**).

$$\Delta_{rxn}G° = -RTlnK_{eq} \qquad \text{Eq. 2}$$

where R is the gas constant (8.314 J mol^{-1} K^{-1}), and T is the Kelvin temperature. Evaluating equilibrium constants allows calculations of the relations among the reactants and products of the reactions in pre-digestion and the anaerobic digesters.

$\Delta_{rxn}G°$ for a reaction under standard conditions is related to $\Delta_{rxn}G$, the Gibbs energy change under non-standard conditions by the relation (**Eq. 3**).

$$\Delta_{rxn}G = \Delta_{rxn}G° + RTlnQ \qquad \text{Eq. 3}$$

where Q is the reaction quotient, i.e., the product of activities of reaction products divided by the product of the activities of reactants with the activity of each species raised to the power of the coefficient in the balanced reaction. This work assumes activities are equal to molar concentrations, i.e., moles of solute per liter of solution. $\Delta_{rxn}G°$ is the driving force for reactions under standard conditions, e.g., when VFA anions, HCO_3^-, and CH_3COO^- concentrations are all 1 mole L^{-1} and H_2(aq) and CO_2(aq) are in equilibrium with a 1-atm partial pressure of each of the gases over the solution. $\Delta_{rxn}G$ is the driving force for reactions under other than standard conditions. If $\Delta_{rxn}G$ is positive, no significant reaction happens. If $\Delta_{rxn}G = 0$, the reaction is at equilibrium, and nothing happens. If $\Delta_{rxn}G$ is negative, the reaction occurs to a significant extent. **Equation 3** shows a reaction with a positive $\Delta_{rxn}G°$ can lead to a negative $\Delta_{rxn}G$ if the reactants are at high concentrations and products are at low concentrations.

In addition to the exozymes synthesized by *C. bescii* for catalyzing hydrolysis reactions, the desired products from both the pre-digestion and digestion phases of MHP, i.e., acetate from pre-digestion and methane from AD, are the products of the catabolic reactions of *C. bescii* and methanogens, respectively. Therefore, in the context of this paper, microorganisms are considered biological catalysts for the reactions. By reducing the activation energy to near zero, catalysts of this type can increase the rates of selected reactions from zero to very fast, but because they are neither reactants nor products, they do not enter into the thermodynamics of the reactions. Because the activation energies for enzyme-catalyzed reactions are small, non-equilibrium thermodynamics shows it is safe to assume the more negative $\Delta_{rxn}G$, the faster the reaction goes, i.e., the reaction rate is proportional to $-\Delta_{rxn}G$. The rate law for enzyme-catalyzed reactions is typically expressed as the Michaelis-Menton/Briggs-Haldane equation (**Eq. 4**).

$$\text{Rate} = d[\text{products}]/dt = k[\text{active enzyme/microorganism}][\text{substrate}]/(K_M + [\text{substrate}]) \qquad \text{Eq. 4}$$

where K_M is an empirical constant and square brackets indicate the concentration of the material, typically number concentrations for enzymes and organisms and molar concentrations for substrates. Note that the rate increases linearly with increasing concentration of the enzyme or microorganism catalyzing the reaction and with increasing concentration of the substrate (the $\Delta_{rxn}G$ effect) until the enzyme or microorganism catabolism is saturated (the K_M + substrate effect).

Achieving high rates in a commercial system thus requires having the right conditions and retention time in the ASB to produce a high steady-state concentration of hydrolysis products and acetate and having the right conditions and retention time for methanogenesis to convert the ASB products into biogas at a high, steady-state rate. Along with concentrations of substrates for methanogenesis, the temperature is critical for achieving high biogas production rates. Rates of catabolic reactions typically double for each 10°C rise in temperature up to the denaturation temperature of the enzyme or organism that catalyzes the reaction. Thermophilic digestion thus has advantages over mesophilic digestion if the digester has the right mix of hydrogen-producing bacteria and methanogens adapted to thermophilic conditions and high substrate loadings. Because of the higher temperature used in pre-digestion, thermophilic digestion is also more energy efficient in the operation of MHP. Enzymes and organisms typically have a 20°C range of activity; the activity rises exponentially over about the lower three-fourths of the range and then decreases rapidly at higher temperatures. Digester temperature thus must be maintained within ±2°C of the optimum to maximize the biogas production rate.

To place the current study in perspective, **Table 3** lists recent, germane research works.

2. Chemical reactions in the microbial hydrolysis process (MHP)

Building a thermodynamic model requires knowledge of the chemical reactions in the system and the states of the chemical species in the reactions. States are indicated by (s) for solids, (l) for liquids, (g) for gases, and (aq) for aqueous. The reactions in the MHP are reasonably well-known (Popovic et al., 2019; Kataeva et al., 2013), as are the reactions of sugars and VFAs in the digester (Schink, 1997; Thauer et al., 1977; Conrad, 1999; Kato and Watanabe, 2010; Lyu et al., 2018). However, the reactions of lignin in AD have not been characterized, and there may be other organic compounds in dairy manure that are as yet unknown.

2.1. Reactions in the anaerobic secretome bioreactor

The following reactions shown by **Equations 5-8** are catalyzed by exozymes from *C. bescii*.

Please cite this article as: Hansen L.D. Thermodynamic method for analyzing and optimizing pretreatment/anaerobic digestion systems. Biofuel Research Journal 38 (2023) 1816-1829. DOI: 10.18331/BRJ2023.10.2.2

Table 3.
References and features of the current study and related works.*

Reference	Features
Qian et al. (2019)	A method using functional exergy efficiency as a unified protocol is proposed to evaluate the effectiveness of energy utilization in three utilization pathways of various biomasses: pyrolysis, oxygen gasification, and AD. The pyrolysis and oxygen gasification processes are simulated by the Gibbs energy minimization method. Biogas data from the AD process are obtained through the PBMP model. The functional exergy efficiencies of utilization pathways of biomasses are evaluated based on the process simulation results. (Note that "exergy" is essentially the same as "Gibbs energy", but exergy analysis only considers the ratio of energy out to energy in, i.e., energy efficiency.)
Skorek-Osikowska (2022)	Mathematical models of mass, energy flow, and gas composition comparing the carbon footprints of biomass gasification and anaerobic digestion is used.
Sinbuathong et al. (2022)	A practical model based on thermodynamic balance equations using Aspen Plus Thermodynamic analysis for AD and the NRTL-RK (Non-Random Two-Liquid) model for properties of liquid and gas phases are employed. Hydrolysis, acidogenesis, acetogenesis, and methanogenesis are used to develop a simulation model (Aspen Plus uses generalized models to estimate properties for engineering design).
Holtzapple et al. (2022)	Describes a "carboxylate platform" that is the purposeful operation of a "stuck" digester that employs a diverse microbial consortium of anaerobes to produce a mixture of C1–C8 monocarboxylic acids and salts. Agricultural residues, municipal solid waste, sewage sludge, animal manure, food waste, algae, and energy crops are considered as feedstocks. This review highlights thermodynamic underpinnings, influences of inoculum source and operating conditions on product formation, and downstream chemical processes that convert the carboxylates to hydrocarbon fuels and oxygenated chemicals.
Bertacchi et al. (2021)	This study modifies the Anaerobic Digestion Model No. 1 (ADM1) describing biomethane production from activated sludge by adding substrate consumption yields in equations describing microbial growth to better reflect the consortium behavior. The work updates the ADM1 model with the microbiology of the process and evaluates which industrially relevant parameters have the most impact on biomethane production. Biochemical reactions from glucose to biomethane are stoichiometrically balanced and analyzed by eQuilibrator with estimated Gibbs free energies (DrG') and equilibrium constants (K'eq) at pH, pMg, and ionic strength values of 7.5, 3.0, and 0.25 M, respectively. [ADM1, Anaerobic Digestion Model No. 1, is an engineering model that uses generalized, steady-state kinetics to describe the AD process (Batstone et al., 2002)].
Current Study	A new pretreatment process that uses *Caldicellulosiruptor bescii* at 75°C for pre-digestion and produces biogas in an anaerobic digester from 5-10% aqueous suspensions of dairy manure naturally buffered at pH 7.8 by ammonium bicarbonate is modeled with thermodynamics. The pre-digestion hydrolyzes lignocellulose and other compounds and produces high concentrations of acetate and anions of VFAs. This study aims to understand the effects of this large influent of VFA anions on the AD system. $\Delta_{rxn}G°$ values are calculated for the major reactions in pre-digestion and reactions producing H_2, acetate, CO_2, and methane in the digester. Curves of $\Delta_{rxn}G$ values *vs.* acetate concentration are used to predict the responses of reactions to increasing acetate and VFA anions and to predict the optimum concentration of acetoclastic methanogens. The method used in this study focuses on Gibbs energies of reactions inside the digester, as opposed to exergy analysis which only looks at Gibbs energies in the input and output. The kinetics of reactions is considered only as relative rates of syntrophic and acetoclastic methanogenesis.

*A Web of Science search with keywords "thermodynamic", "anaerobic digestion", and "manure" for the period 2018-2023 produced eight references, five of which were germane to the current study.

Cellulose:

$$(C_6H_{10}O_5)_n(s) + nH_2O(l) \rightarrow nC_6H_{12}O_6(aq) \quad \text{Eq. 5}$$

Esters:

$$RCOOR(aq)' + OH^-(aq) \rightarrow RCOO^-(aq) + R'OH(aq) \quad \text{Eq. 6}$$

Amides:

$$RCONHR'(aq) + H_2O(l) \rightarrow RCOO^-(aq) + R'NH_3^+(aq) \text{ or amino acids, } R(NH_3^+)COO^-(aq) \quad \text{Eq. 7}$$

Amino acids:

$$R(NH_3^+)COO^-(aq) + H_2O(l) \rightarrow R(OH)COO^-(aq) + NH_4^+(aq) \quad \text{Eq. 8}$$

While the reactions presented by **Equations 9-12** are catabolic reactions of *C. bescii*.

Glucose:

$$C_6H_{12}O_6(aq) + 3HCO_3^-(aq) \rightarrow 3CH_3COO^-(aq) + 3CO_2(aq) + 3H_2O(l) \quad \text{Eq. 9}$$

$$C_6H_{12}O_6(aq) + 3CO_3^{2-}(aq) \rightarrow 3CH_3COO^-(aq) + 3HCO_3^-(aq) \quad \text{Eq. 10}$$

$$C_6H_{12}O_6(aq) + 2HCO_3^-(aq) \rightarrow 2CH_3CH(OH)COO^-(aq) + 2CO_2(aq) + 2H_2O(l) \quad \text{Eq. 11}$$

$$C_6H_{12}O_6(aq) + 2CO_3^{2-}(aq) \rightarrow 2CH_3CH(OH)COO^-(aq) + 2HCO_3^-(aq) \quad \text{Eq. 12}$$

The reactions shown in **Equations 10**, **11**, and **12** are unlikely given the low concentration of carbonate ion at pH 7.8 (see **Table 5**) and the lack of evidence for lactate in the system but are included for completeness. Note that $CO_2(aq)$ includes both $CO_2(aq)$ and $H_2CO_3(aq)$.

2.2. Syntrophic methanogenesis reactions in anaerobic digestion

The reactions presented by **Equations 13-19** produce H_2 and acetate from VFA anions by hydrogen-producing syntrophic bacteria.

Iso-valerate:

$$CH_3CH(CH_3)CH_2COO^-(aq) + 2HCO_3^-(aq) \rightarrow 3CH_3COO^-(aq) + H_2(aq) + CO_2(aq) \quad \text{Eq. 13}$$

2-Methylbutyrate:

$$CH_3CH_2CH(CH_3)COO^-(aq) + 2HCO_3^-(aq) \rightarrow 3CH_3COO^-(aq) + H_2(aq) + CO_2(aq) \quad \text{Eq. 14}$$

n-Valerate:

$$CH_3CH_2CH_2CH_2COO^-(aq) + 2HCO_3^-(aq) \rightarrow 3CH_3COO^-(aq) + H_2(aq) + CO_2(aq) \quad \text{Eq. 15}$$

Iso-butyrate:

$$CH_3CH(CH_3)COO^-(aq) + H_2O(l) + HCO_3^-(aq) \rightarrow 2CH_3COO^-(aq) + 2H_2(aq) + CO_2(aq) \quad \text{Eq. 16}$$

n-Butyrate:

$$CH_3CH_2CH_2COO^-(aq) + H_2O(l) + HCO_3^-(aq) \rightarrow 2CH_3COO^-(aq) + 2H_2(aq) + CO_2(aq) \quad \text{Eq. 17}$$

Propionate:

$$CH_3CH_2COO^-(aq) + 2H_2O(l) \rightarrow CH_3COO^-(aq) + 3H_2(aq) + CO_2(aq) \quad \text{Eq. 18}$$

Please cite this article as: Hansen L.D. Thermodynamic method for analyzing and optimizing pretreatment/anaerobic digestion systems. Biofuel Research Journal 38 (2023) 1816-1829. DOI: 10.18331/BRJ2023.10.2.2

Acetate:

$CH_3COO^-(aq) + 3H_2O(l) \rightarrow HCO_3^-(aq) + CO_2(aq) + 4H_2(aq)$ Eq. 19

Note that $CO_2(aq)$ includes both $CO_2(aq)$ and $H_2CO_3(aq)$. Also, note that hydrogen production from acetate requires a different species of hydrogen-producing bacteria than longer-chain VFAs. The reaction shown by **Equation 20** produces methane from the catabolic reaction of syntrophic methanogens.

$4H_2(aq) + CO_2(aq) \rightarrow CH_4(g) + 2H_2O(l)$ Eq. 20

Equation 21 presents the reaction producing methane from the catabolic reaction of acetoclastic methanogens.

Acetate:

$CH_3COO^-(aq) + H_2O(l) \rightarrow HCO_3^-(aq) + CH_4(g)$ Eq. 21

3. Thermodynamic data

Table 4 gives the pK_a values and ionic states at 25°C for the common acids and bases found in the digestion of dairy manure. The carboxylic and amino acids are in the same ionic state at the higher temperatures in the ASB (75°C) and AD (40 or 55°C), but the states of carbonic acid and ammonium ion vary significantly with temperature. **Table 5** gives the ratios of base/acid for carbonic acid and ammonia at 25, 40, 55, and 75°C. **Table 6** tabulates the thermodynamic values of the standard Gibbs energy, $\Delta_fG°$, and where available, enthalpy, $\Delta_fH°$, entropy, S°, and heat capacity, $C_p°$, for the reaction for the formation of each of the compounds and ions in their standard state from the elements in their standard state. The $\Delta_fH°$, S°, and $C_p°$ values can be used to calculate $\Delta_fG°$ values at other temperatures. However, note that $\Delta_fH°$, S°, and $C_p°$ values are not available for the anions of VFAs, and therefore the temperature dependence of reactions involving these species cannot be calculated.

4. Results and Discussion

4.1. Standard Gibbs energy changes and equilibrium constants for reactions

Table 7 presents standard Gibbs energy changes for the major reactions in the ASB, while **Table 8** gives standard Gibbs energy changes for reactions producing H_2, acetate, and CO_2 in the anaerobic digester. **Table 9** tabulates standard Gibbs energy changes for methanogenesis reactions in the digesters. **Table 10** provides standard Gibbs energy changes for directly coupled reactions of syntrophic methanogenesis.

Figure 2 shows a plot of $\Delta_{rxn}G°(25°C)$ for β-oxidation of VFA anions to produce $H_2(aq)$ and acetate(aq), i.e., reactions shown in **Equations 16-19**. Note that the value of $\Delta_{rxn}G°(25°C)$ becomes less positive as chain length increases by -45.6 kJ $mole^{-1}$ CH_2 $group^{-1}$. This constant value of the slope may be a consequence of the way Thauer et al. (1977) determined the values of $\Delta_fG°$ for the aqueous anions. Extrapolation of the fitted line to more than five C atoms suggests that $\Delta_{rxn}G°(25°C)$ would approach zero at caproate; however, more likely the value of $\Delta_{rxn}G°(25°C)$ levels off to a constant positive value around 20 kJ mol^{-1} of reaction.

To obtain a significant reaction for a reaction with a large positive $\Delta_{rxn}G°$, such as the reactions in **Table 8**, the reaction can be coupled with another reaction that uses the products of the first reaction in a reaction with a larger negative $\Delta_{rxn}G°$, such as the syntrophic reaction presented in **Equation 20** in **Table 9**. Coupling can occur either indirectly or directly. Indirectly coupled reactions do not have a fixed stoichiometry because some of the intermediates are lost and not taken up by the second reaction. Directly coupled reactions have a fixed stoichiometry with whole-number coefficients. The type of coupling between hydrogen-producing bacteria and hydrogenotrophic methanogens is unknown and may vary depending on how tight the symbiotic relationship is. The H_2-producing reactions of syntrophic methanogenesis from the anions of the short-chain carboxylic acids considered here all have positive $\Delta_{rxn}G°$ values, which decrease in the order, acetate > propionate > butyrate > valerate (see **Table 8**) and can produce only very low concentrations of hydrogen. If the bacteria-produced hydrogen is dissolved in the solution and then taken up by a syntrophic methanogen, i.e., by indirect coupling, methanogenesis will occur very slowly. But, because the rate of syntrophic methanogenesis is relatively rapid, it is a likely conclusion that the hydrogen-producing bacteria and the methanogen are directly coupled, probably in a biofilm. The absence of hydrogen in the biogas also suggests a direct coupling between the bacteria and syntrophic methanogens. $\Delta_{rxn}G°(25°C)$ values for the directly coupled reactions are given in **Table 10**. The $\Delta_{rxn}G°$ values for the coupled methanogenesis/H_2-producing reactions are increasingly negative for acetate, valerate, butyrate, and propionate, in that order.

Table 4.
Species of acids and bases in aqueous solution at 25°C and pH 7.8.*

Chemical Compound	Acetic Acid	Propionic Acid	Butyric & Isobutyric Acids	Valeric & Isovaleric Acids	Caproic & Isocaproic Acids	Lactic Acid	Amino Acids	Carbonic Acid[a]	Ammonium Ion
pK_a (25°C)	4.76	4.87	4.82, 4.87	4.82, 4.87	4.88, 5.09	3.86	2.3, 9.6	6.37, 10.32	9.25
Ionic charge at pH 7.8	-1	-1	-1	-1	-1	-1	±	Mostly -1[a]	Mostly +1[a]

* Source of data: Christensen et al. (1976).
[a] "Carbonic acid" includes both CO_2 (aq) and H_2CO_3(aq).

Table 5.
Speciation of carbonic acid and ammonium ion at pH 7.8 as a function of temperature.

T (°C)	H_2CO_3[a] pK_1[b]	HCO_3^- pK_2[b]	$[HCO_3^-]/[H_2CO_3]$	$[CO_3^{2-}]/[HCO_3^-]$	NH_4^+ pK[c]	$[NH_3]/[NH_4^+]$
25	6.351	10.329	28.1	0.002958	9.245	0.0359
40	6.222	10.086	37.8	0.005176	8.805	0.0989
55	6.108	9.862	49.2	0.00867	8.415	0.243
75	5.977	9.587	66.5	0.0163	7.971	0.674

[a] Note that H_2CO_3 includes both H_2CO_3 and CO_2(aq).
[b] **Equations 6** and **7** from Millero et al. (2002), corrected to agree with Goldberg et al. (2002), at 25°C gave $pK_1 = 2.8243x10^{-5}T^2 - 0.01029T + 6.5890$ and $pK_2 = 3.3425x10^{-5}T^2 - 0.018157T + 10.760$. T is in °C.
[c] Goldberg et al. (2002). The equation obtained from fitting the data is $pK = 1.1007T^2 - 3.6480T + 10.088$. T is in °C.

4.2. Effects of acetate concentration on anaerobic digestion

Acetate is one of the main products of pre-digestion and is the common product and reactant in many of the reactions in the digester. Therefore, acetate concentration is used as the common variable in analyzing reactions in the digester. In the digestion of dairy manure by the MHP, there are two sources of acetate, the manure and pre-digestion, with roughly equal amounts, although some observations suggest twice as much comes from

Please cite this article as: Hansen L.D. Thermodynamic method for analyzing and optimizing pretreatment/anaerobic digestion systems. Biofuel Research Journal 38 (2023) 1816-1829. DOI: 10.18331/BRJ2023.10.2.2

Table 6.
Thermodynamic values of the standard Gibbs energy, $\Delta_f G°$, and where available, enthalpy, $\Delta_f H°$, entropy, S°, and heat capacity, $C_p°$, for the reaction for the formation of each of the compounds and ions in their standard state from the elements in their standard states at 25°C.

Compound or Ion	$\Delta_f G°$, kJ mol^{-1}	$\Delta_f H°$, kJ mol^{-1}	S°, J mol^{-1} K^{-1}	$C_p°$, J mol^{-1} K^{-1}	Reference
H_2(aq)	+17.6	-4.2	57.7	-	
H_2(g)	0	0	130.684	28.824	
H^+(aq)	0	0	0	0	
O_2(g)	0	0	205.138	29.355	
CO_2(aq)	-385.98	-413.80	117.6	-	Wagman et al. (1982)
CO_2(g)	-394.359	-393.509	213.74	-	
H_2O(l)	-237.129	-285.830	69.91	75.291	
HCO_3^-(aq)	-586.77	-691.99	91.2	-	
CO_3^{2-}(aq)	-527.81	-677.14	-56.9	-	
CH_3COO^-(aq)	-369.31 -369.0	-486.01 -486.0	86.6 85.3	-6.3	Wagman et al. (1982); Miller and Smith-Magowan (1990)
CH_4(g)	-50.72	-74.81	186.264	-	
CH_4(aq)	-34.33	-89.04	83.7	-	Wagman et al. (1982)
NH_4^+(aq)	-79.31	-132.51	113.4	79.9	
NH_3(aq)	-26.5	-80.29	111.3	-	
$C_6H_{12}O_6$(aq)	-917.22	-	-	-	Thauer et al. (1977)[a]
$(C_6H_{10}O_5)_n$(s)	-[b]	-	-	-	Popovic et al. (2019)[b]
$CH_3CH_2COO^-$(aq)	-361.08	-	-	-	Thauer et al. (1977)[a]
$CH_3CH_2CH_2COO^-$(aq)	-352.63	-	-	-	
$CH_3CH(CH_3)COO^-$(aq)	NA	-	-	-	-
$CH_3CH_2CH_2CH_2COO^-$(aq)	-344.34	-	-	-	Thauer et al. (1977)[a]
$CH_3CH_2CH(CH_3)COO^-$(aq)	NA	-	-	-	-
$CH_3CH(CH_3)CH_2COO^-$(aq)	NA	-	-	-	-
$CH_3CH(OH)COO^-$(aq)	-517.81	-686.2	-	-	Thauer et al. (1977)[a]; Miller and Smith-Magowan (1990)
$NH_3^+CH_2COO^-$(aq)	-370.647 -371.20	-513.988 -514.36	158.32 158.45	-	Wagman et al. (1982); Miller and Smith-Magowan (1990)
CH3 $NH_3^+CH_2COO^-$(aq)	-371.54 -370.50	-553.75 -553.75	159.80 159.80	-	Thauer et al. (1977)[a]; Miller and Smith-Magowan (1990)

[a] **Table 15**.
[b] This reference gives values for $\Delta_f G^\circ$, $\Delta_f H^\circ$, S°, and Cp° are as functions of temperature.

pre-digestion than from the manure. **Table 11** gives the composition of the steady-state solution in AD considered here. For calculation purposes, the steady-state acetate(aq) concentration in AD is varied from 100 to 15,000 mg/L (254 to 1.7 mM). The concentrations of HCO_3^-(aq), CO_2(aq), partial pressure of CH_4 (P_{CH4}), and the concentrations of propionate(aq), butyrate(aq), and valerate(aq) are assumed constant in the steady-state conditions.

4.2.1. Effect of acetate concentration on biogas production by indirectly coupled syntrophic methanogenesis

The equations for syntrophic methanogenesis are shown in **Equation 22**.

$$4H_2(aq) + CO_2(aq) \rightarrow CH_4(g) + 2H_2O(l) \quad \text{Eq. 22}$$

$\Delta_{rxn}G° = -209$ kJ mol^{-1} and $K_{eq} = 4.8x10^{36} = P_{CH4}/[H_2]^4[CO_2]$

Assuming the concentrations of HCO_3^-, CO_2(aq), P_{CH4}, and VFA anions as given in **Table 11**, **Equation 22** is at equilibrium when $[H_2(aq)] = 1.2x10^{-9}$ M. (Note M = mole L^{-1} and is indicated by square brackets). If $[H_2(aq)]$ is greater than $1.2x10^{-9}$ M, the reaction in **Equation 21** is downhill, and the greater the $[H_2(aq)]$, the faster the reaction will go. Reactions presented in **Equations 13-18** produce acetate, H_2(aq), and CO_2(aq), while those shown in **Equations 12-16** consume bicarbonate, and reaction in **Equation 18** consumes acetate to make bicarbonate, CO_2(aq) and hydrogen. The $\Delta_{rxn}G°(25°C)$ values and equilibrium constant functions are given in **Table 8**. Because $\Delta_{rxn}G°$ is positive for all of the reactions, none of the reactions will happen to a significant extent under standard

Please cite this article as: Hansen L.D. Thermodynamic method for analyzing and optimizing pretreatment/anaerobic digestion systems. Biofuel Research Journal 38 (2023) 1816-1829. DOI: 10.18331/BRJ2023.10.2.2

Table 7.
Standard Gibbs energy changes at 25°C for the reactions in the ASB at pH 7.8.*

Reaction in Equation #	$\Delta_{rxn}G°(25°)$, kJ mol^{-1}	K_{eq}	Remarks
5 Cellulose	-	= $[C_6H_{12}O_6]$	Cellulose hydrolysis is driven to completion by the very high solubility of glucose which increases as temperature increases.
6 Esters	-	= $[RCOO^-][R'OH]/[RCOOR'][OH^-]$	Ester linkages in lignin are hydrolyzed, giving insoluble products. Esters in lipids are hydrolyzed to soluble alcohols and VFA anions.
7 Amides	-	= $[R(NH_3^+)COO^-]/[RCONHR']$	Protein, except that in *C. bescii* and exozymes, is completely hydrolyzed to amino acids.
8 Amino acids	+11.45	9.9×10^{-3} = $[R(OH)COO^-][NH_4^+]/[R(NH_3^+)COO^-]$	Amino acids may be hydrolyzed to an α-hydroxy amino acid and ammonium ion. An example is for alanine to lactate.
9 Glucose	-299.73	3.3×10^{52} = $[CH_3COO^-]^3[CO_2]^3/[C_6H_{12}O_6][HCO_3^-]^3$	Note the third-order dependence on bicarbonate protonation that drives this catabolic reaction for the growth of *C. bescii*.
10 Glucose	-367.59	2.5×10^{64} = $[CH_3COO^-]^3[HCO_3^{2-}]^3/[C_6H_{12}O_6][CO_3^{2-}]^3$	Possible reaction, but unlikely because of the very low carbonate concentration.
11 Glucose	-191.18	3.1×10^{33} = $[CH_3CH(OH)COO^-]^2[CO_2]^2/[C_6H_{12}O_6][HCO_3^-]^2$	Note the second-order dependence on bicarbonate protonation that drives this catabolic reaction, but not as energetically productive as the reaction shown in Equation 9.
12 Glucose	-236.32	2.5×10^{41} = $[CH_3CH(OH)COO^-]^2[HCO_3^{2-}]^2/[C_6H_{12}O_6][CO_3^{2-}]^2$	Also not likely because of the very low carbonate concentration.

* Square brackets indicate molar concentrations of aqueous species. The standard state of gases is 1 bar. The activity of H_2O(l) and solids (cellulose and lignin) is assumed to be 1. The data are for reactions at 25°C, but the reactions in the ASB occur at 75°C. Values for S° of aqueous glucose, alanine, and lactate would be necessary to determine the temperature correction for reactions presented in **Equations 8-12**.

Table 8.
Standard Gibbs energy changes at 25°C for the reactions in the ASB at pH 7.8.[a]

Reaction in Equation #	$\Delta_{rxn}G°(25°C)$, kJ mol^{-1}	K_{eq}
13 iso-valerate[a]	-	= $[CH_3COO^-]^3[H_2][CO_2]/[CH_3CH(CH_3)CH_2COO^-][HCO_3^-]^2$
14 2- methylbutyrate[a]	-	= $[CH_3COO^-]^3[H_2][CO_2]/[CH_3CH_2CH(CH_3)COO^-][HCO_3^-]^2$
15 n-valerate[b]	+41.57	5.2×10^{-8} = $[CH_3COO^-]^3[H_2][CO_2]/[CH_3CH_2CH_2CH_2COO^-][HCO_3^-]^2$
16 iso-butyrate[a]	-	= $[CH_3COO^-]^2[H_2]^2[CO_2]/[CH_3CH(CH_3)COO^-][HCO_3^-]$
17 n-butyrate[b]	+87.13	5.4×10^{-16} = $[CH_3COO^-]^2[H_2]^2[CO_2]/[CH_3CH_2CH_2COO^-][HCO_3^-]$
18 Propionate[b]	+132.85	5.3×10^{-24} = $[CH_3COO^-][H_2]^3[CO_2]/[CH_3CH_2COO^-]$
19 Acetate	+178.35(25°C) +176.20(40°C) +174.05(55°C)	5.7×10^{-32}(25°C), 1.4×10^{-31}(40°C), 3.2×10^{-31}(55°C) = $[HCO_3^-][CO_2][H_2]^4/[CH_3COO^-]$

[a] The $\Delta_{rxn}G°(25°C)$ and associated K_{eq} values for iso-valerate and 2-methylbutyrate are likely very close to the values for n-valerate, and the values for iso-butyrate are likely very close to the values for n-butyrate.
[b] The values of $\Delta_{rxn}G°$ at 40 and 55°C for the reactions shown in **Equations 13-18** probably follow the same trend with temperature as the values for acetate, the reaction in **Equation 19**, i.e., becoming less positive with increasing temperature.

conditions. Also, note that $\Delta_{rxn}G°$ becomes more positive as the VFA hydrocarbon chain gets shorter. However, $\Delta_{rxn}G$ (without the °) is the driving force for reactions under other than standard conditions, **Equation 3**. If $\Delta_{rxn}G = 0$, the reaction is at equilibrium, and nothing happens. If $\Delta_{rxn}G$ is positive, the reaction is uphill, produces less product, and runs slower. If $\Delta_{rxn}G$ is negative, the reaction is downhill, produces more product, and runs faster. Only downhill reactions can happen to any significant extent in AD. The equilibrium concentrations of [H_2(aq)] that can be made by the hydrogen-producing bacteria are calculated as a function of the concentration of acetate, [CH3COO$^-$], and with the concentrations of propionate, butyrate, and valerate in **Table 11**. The results are depicted in **Figure 3**.

Please cite this article as: Hansen L.D. Thermodynamic method for analyzing and optimizing pretreatment/anaerobic digestion systems. Biofuel Research Journal 38 (2023) 1816-1829. DOI: 10.18331/BRJ2023.10.2.2

Table 9.
Gibbs energy changes for methanogenesis reactions at pH 7.8. The values of $\Delta_{rxn}G°$ given are calculated from data at 25°C and corrected to 40 and 55°C by use of the relation, $d(\Delta_{rxn}G°)/dT = -\Delta_{rxn}S°(25°C)$, assuming the entropy change is constant with temperature.

Reaction in Equation #	$\Delta_{rxn}G°$(25°C), kJ mol^{-1} K_{eq}	$\Delta_{rxn}G°$(40°C), kJ mol^{-1} K_{eq}	$\Delta_{rxn}G°$(55°C), kJ mol^{-1} K_{eq}	K_{eq}
20 Syntrophic	-209.40 4.8×10^{36}	-209.7 5.5×10^{36}	-210.0 6.2×10^{36}	$= P_{CH4}/[H_2]^4[CO_2]$
21 Acetoclastic	-31.05 2.8×10^{5}	-32.85 5.7×10^{5}	-34.65 12×10^{5}	$= [HCO_3^-]P_{CH4}/[CH_3COO^-]$

Table 10.
$\Delta_{rxn}G°(25°)$ and K_{eq} for directly coupled reactions of syntrophic methanogenesis.

Substrate	$\Delta_{rxn}G°$(25°), kJ mol^{-1}	K_{eq}
iso-valerate	-	-
2-methylbutyrate	-	-
n-valerate	-43.12	$3.6\times10^{7} = [CH_3COO^-]^{12}[CO_2]^3P_{CH4}/[CH_3CHCH_2CH_2COO^-]^4[HCO_3^-]^8$
Iso-butyrate	-	-
n-butyrate	-35.14	$1.4\times10^{6} = [CH_3COO^-]^4[CO_2]P_{CH4}/[CH_3CH_2CH_2COO^-]^2[HCO_3^-]^2$
Propionate	-96.80	$9.1\times10^{-16} = [CH_3COO^-]^4[CO_2]P^3_{CH4}/[CH_3CH_2COO^-]^4$
Acetate	-31.05	$2.8\times10^{5} = [HCO_3^-]P_{CH4}/[CH_3COO^-]$

Table 11.
Typical composition of the steady-state solution in AD with pre-digestion of dairy manure.

Chemical species	HCO_3^-(aq)	CO_2 (aq)	P_{CH4}	Propionate (aq)	Butyrate (aq)	Valerate (aq)
Concentration, mg L^{-1}	2500[a]	96	-	1000	100	50
Concentration, mM	50	2	0.02 atm	13.7	1.15	0.50

[a] Alkalinity as $CaCO_3$ equivalents is 2500 mg L^{-1}, but note that the procedures given in Baird et al. (2017) include VFA anions in alkalinity, so Baird alkalinity for this example ≈ 3267 mg $CaCO_3$ L^{-1}.

The concentration of H_2(aq) must be above the dashed line [log(1.2×10^{-9})] in **Figure 3** to get significant syntrophic methanogenesis to occur. Under the specified conditions, only acetate, propionate, and valerate allow syntrophic methanogenesis to occur to any significant extent. Butyrate can supply sufficient H_2(aq) only if $[CH_3COO^-]$ < 200 mg L^{-1}. Increasing acetate concentration increases $[H_2(aq)]$ from acetate as the fourth root of the concentration of acetate, so increasing acetate increases H_2(aq) from acetate very little. Because acetate is a byproduct of hydrogen production from valerate, butyrate, and propionate, increasing acetate increasingly inhibits hydrogen production from these VFAs. Therefore, as expected, the rate of hydrogen production decreases as acetate increases, and consequently, biogas production from indirectly coupled syntrophic methanogenesis slows as acetate increases.

4.2.2. Effect of acetate concentration on the rate of directly coupled syntrophic methanogenesis

The reactions for directly coupled syntrophic methanogenesis are presented in the following equations (**Eqs. 23-26**)

$$4CH_3CH_2CH_2CH_2COO^-(aq) + 8HCO_3^-(aq) \rightarrow 12CH_3COO^-(aq) + 3CO_2(aq) + CH_4(g) + 2H_2O(l) \quad \text{Eq. 23}$$

$$2CH_3CH_2CH_2COO^-(aq) + 2HCO_3^-(aq) \rightarrow 4CH_3COO^-(aq) + CO_2(aq) + CH_4(g) \quad \text{Eq. 24}$$

$$4CH_3CH_2COO^-(aq) + 2H_2O(l) \rightarrow 4CH_3COO^-(aq) + CO_2(aq) + 3CH_4(g) \quad \text{Eq. 25}$$

$$CH_3COO^-(aq) + H_2O(l) \rightarrow HCO_3^-(aq) + CH_4(g) \quad \text{Eq. 26}$$

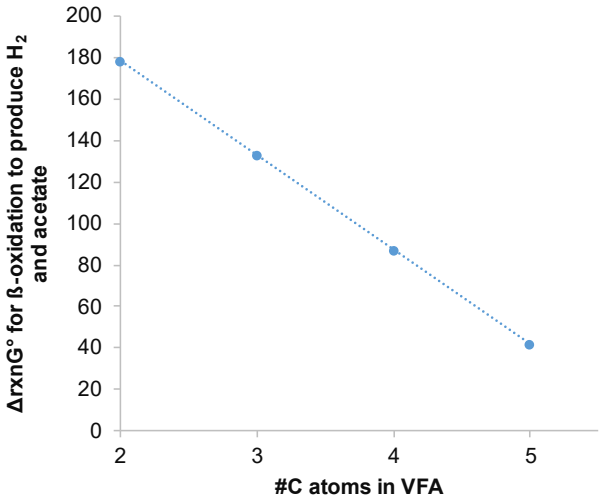

Fig. 2. The plot of $\Delta_{rxn}G°(25°C)$ for β-oxidation of VFAs to produce H_2(aq), CO_2(aq), and acetate(aq), i.e., the reactions presented in **Equations 13-19**.
structures

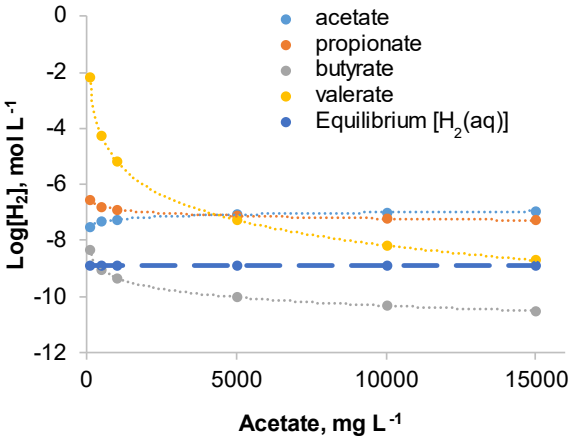

Fig. 3. Logrithmn of the molar concentration of H_2(aq) at equilibrium for VFAs. The equilibrium limit is for the reaction shown in **Equation 22**.

Figure 4 shows the $\Delta_{rxn}G(25°)$ values for directly coupled syntrophic methanogenesis as a function of acetate concentration. Under the specified conditions, syntrophic methanogenesis is significant, i.e., $\Delta_{rxn}G$ is negative

Please cite this article as: Hansen L.D. Thermodynamic method for analyzing and optimizing pretreatment/anaerobic digestion systems. Biofuel Research Journal 38 (2023) 1816-1829. DOI: 10.18331/BRJ2023.10.2.2

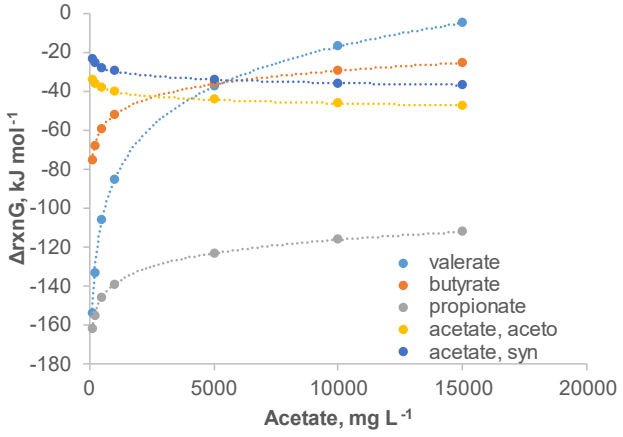

Fig. 4. $\Delta_{rxn}G$ for directly coupled syntrophic methanogenesis.

at all acetate concentrations. However, the reactions rapidly become less favorable as acetate concentration increases. Compared with methanogenesis from acetate, only propionate produces methane more rapidly at higher acetate concentrations.

4.2.3. Effect of acetate concentration on biogas production by acetoclastic methanogenesis

Figure 5 gives the $\Delta_{rxn}G(40°C)$ for direct acetoclastic methanogenesis, the reaction in Equation 21, and syntrophic methanogenesis, the reaction in Equation 20, limited by the concentration of $H_2(aq)$ that can be produced from acetate under the specified conditions. The data show the acetoclastic methanogenesis reaction is expected to be significantly faster than the syntrophic methanogenesis reaction at all acetate concentrations (aq) >100 mg L^{-1}.

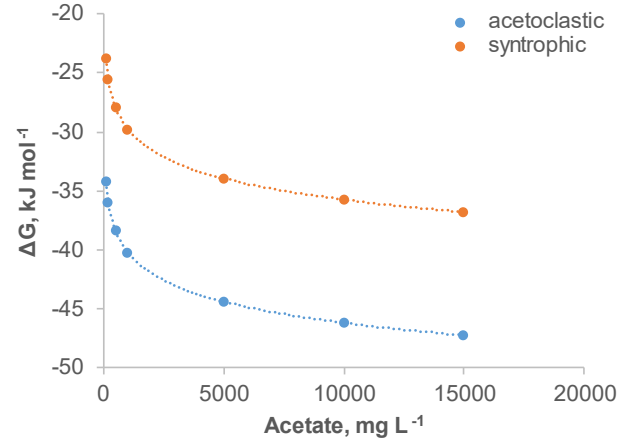

Fig. 5. $\Delta_{rxn}G$ for the direct acetoclastic and directly coupled syntrophic methanogenesis reactions with hydrogen produced from acetate.

4.3. Kinetics of acetoclastic versus syntrophic methanogenesis

The overall methanogenesis reaction of acetate is shown in Equation 27.

$$CH_3COO^-(aq) + H_2O(l) \rightarrow CH_4(g) + HCO_3^-(aq) \quad \text{Eq. 27}$$

The rate law expressed as a function of reactants or products, neglecting the K_M+[substrate] term in the denominator, is presented in Equation 28.

$$d\alpha_t/dt = -k[CH_3COO^-(aq)][microorganism] = k[HCO_3(aq)][microorganism] \quad \text{Eq. 28}$$

where [microorganism] is the number concentration of the rate-limiting organism. For acetoclastic methanogenesis, it is the acetoclastic microorganism, and for syntrophic methanogenesis, it could be either the hydrogen-producing bacteria or the syntrophic methanogen, whichever is rate-limiting. The thermodynamics in Figures 3 and 4 suggest it is most likely the hydrogen-producing bacteria. Equation 28 shows the rate can be measured in a batch system either as the rate of decrease of acetate or the rate of increase of bicarbonate. In a digester running in a steady state, these concentrations are constant inside the digester, and the kinetics can only be obtained from the decrease in acetate and/or increase in bicarbonate between the input and effluent of the digester.

Assuming the concentration of the microorganism is constant, the rate law for the rate of acetate methanogenesis can be written as a function of time, t, as shown in Equation 29.

$$(n_t/n_0) = \alpha_t = e^{-kt} \quad \text{Eq. 29}$$

where n is the concentration of acetate. This equation can be used to obtain the kinetics for methanogenesis in the digester if the digester is assumed to be in a steady state. Because $\Delta_{rxn}G$ is a linear function of ln[acetate] for both acetoclastic and syntrophic methanogenesis, $\Delta_{rxn}G$ can be used to estimate the instantaneous relative rate as a function of acetate concentration. Using the thermodynamics of the steady state (Denbigh, 1951) and assuming direct coupling of syntrophic methanogenesis, Equation 30 can be developed.

$$d[acetate]/dt = \Delta_{rxn20}G[Ac] + \Delta_{rxn1819}G[Syn] \quad \text{Eq. 30}$$

where $\Delta_{rxn21}G$ is for the reaction presented in Equation 21, $\Delta_{rxn1920}G$ is for the combination of reactions presented in Equations 19 and 20, [Ac] is the number concentration of acetoclastic methanogens, and [Syn] is the number concentration of either the syntrophic bacteria or the syntrophic methanogen.

Assuming [Ac] = [Syn] = constant, the time required to convert a fixed amount of acetate into products in a steady-state reaction is directly proportional to $-\Delta_{rxn}G^{-1}$, i.e., $dt = d[acetate]/\Delta_{rxn20}G[Ac]$ or $dt = d[acetate]/\Delta_{rxn1819}G[Syn]$. Figure 6 shows the results of these calculations for acetoclastic and syntrophic methanogenesis. Although $\Delta_{rxn}G°$ is the same for the reaction shown in Equation 27 for acetoclastic and syntrophic methanogenesis, syntrophic methanogenesis is slower because of the dependence on the rate of production of $H_2(aq)$ as an intermediate.

The data in Figure 6 have the same form as the rate of decay of a reactant in a first-order reaction, i.e., Equation 29. Therefore, plotting the data as $\ln(\alpha_t)$, where α_t equals the initial acetate concentration in Figure 7 *vs.* relative time, gives an estimate of the rate constant, k, as the slope. The results show that, under identical steady-state conditions, acetoclastic methanogenesis runs about 1.4 times faster than syntrophic methanogenesis.

4.4. Predicting the performance of dairy manure digestion

The reaction model of the MHP system given in Table 2 and the information in the above discussion can be used to predict the performance of dairy manure digestion with and without pre-digestion and with differing methanogen cultures. Pre-digestion significantly increases acetate and probably increases other VFA anions in the AD feed, but for comparison purposes, the concentrations of propionate, butyrate, and valerate are held constant at the same concentrations used in the calculations based on Table 11. Table 12 gives the assumed acetate and other VFA concentrations in the steady state influent to AD with and without pre-digestion. Table 13 provides the estimated AD performance for various concentrations of acetoclastic methanogens. Syntrophic methanogenesis is assumed to completely convert all VFAs except acetate to biogas. The conversion of acetate is assumed to be proportional to the acetoclastic methanogen

Please cite this article as: Hansen L.D. Thermodynamic method for analyzing and optimizing pretreatment/anaerobic digestion systems. Biofuel Research Journal 38 (2023) 1816-1829. DOI: 10.18331/BRJ2023.10.2.2

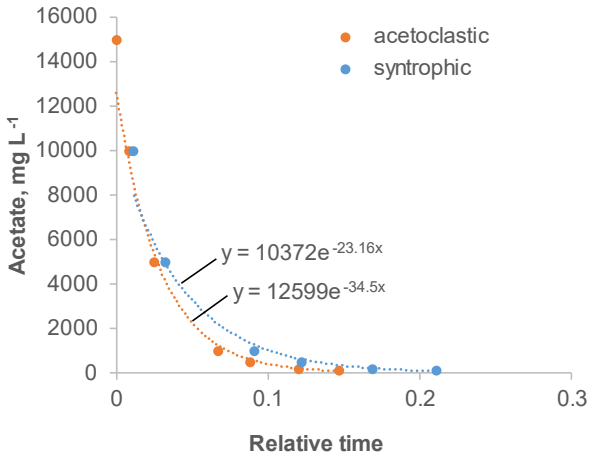

Fig. 6. The relative time for the reaction of a fixed amount of acetate as a function of the acetate concentration.

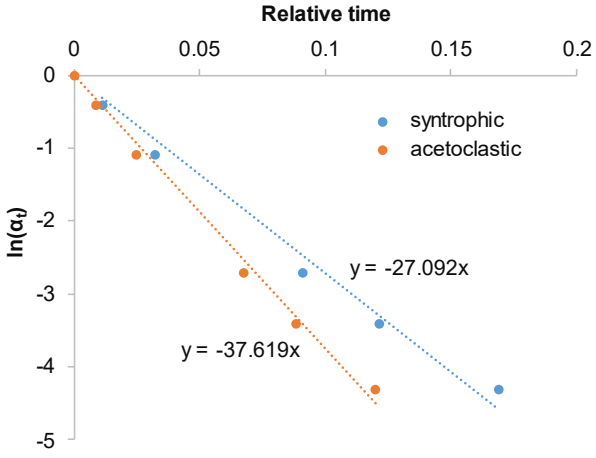

Fig. 7. Rate constants for syntrophic and acetoclastic methanogenesis estimated from the slopes of the lines.

Table 12.
The relative effect of AD influent composition on methane production.

Anion	Pre-digestion input (MHP), mg L^{-1}	No pre-digestion, mg L^{-1}
Acetate	15000	5000
Propionate	1000	1000
Butyrate	100	100
Valerate	50	50

concentration. As a reference, we assume a sufficiently long retention time and the right mix of methanogenesis in AD to achieve complete digestion of all VFAs, including acetate. **Figure 8** provides a visual representation of the effects of pre-digestion and acetoclastic methanogen concentration on digester performance at producing methane.

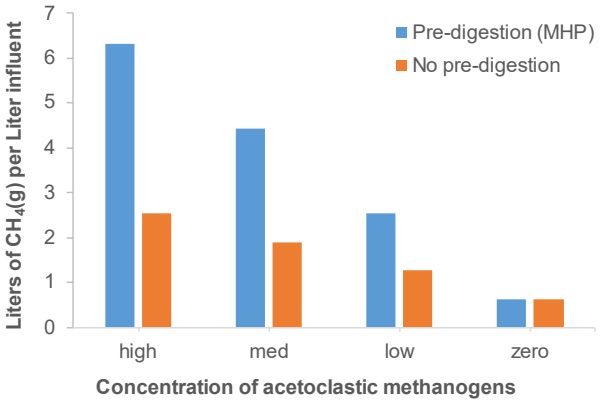

Fig. 8. Effect of pre-digestion, blue bars *vs.* red bars, and acetoclastic methanogen concentration on methane production from dairy manure.

4.5. Determination of steady-state conditions in a digester

Note that most of the results depend on the steady-state conditions in the digester, i.e., the pressure of $CH_4(g)$ and the concentrations of $HCO_3^-(aq)$, $CO_2(aq)$, acetate, propionate, butyrate, and valerate (see **Table 11** for the values assumed for this study). $CH_4(g)$ and $CO_2(aq)$ can be estimated from the partial pressures of methane and carbon dioxide in the biogas, which is commonly measured. However, the rapid test methods that are available for VFAs and alkalinity determine total carboxylate concentration (Hach kit product #2244700) and total alkalinity as the sum of $HCO_3^-(aq)$ and base equivalents of VFAs (Baird et al., 2017). The alkalinity measured according to Baird et al. (2017) gives the sum [bicarbonate + VFAs] as mg $CaCO_3$ L^{-1}. The Hach kit for VFAs gives the sum of all the VFAs as mg CH_3COO^- L^{-1}. The Baird alkalinity and Hach VFAs can be combined to estimate HCO_3^-, as shown in **Equations 31-33**.

(X mg L^{-1} $CaCO_3$)(1 mmol 100 mg^{-1})(2 meq alk $mmol^{-1}$) = (X/50) Baird meq alk L^{-1} Eq. 31

(Y mg Hach CH_3COO^-)(1 mmol 63 mg^{-1})(1 meq alk $mmol^{-1}$) = (Y/63) Hach meq alk L^{-1} Eq. 32

[(X/50) – (Y/63)](61 mg HCO_3^- meq alk^{-1}) ≈ mg HCO_3^- L^{-1} Eq. 33

VFA speciation must be done to determine the individual concentrations of each of the VFAs. Pind et al. (2003b) describe a definitive method for VFA speciation in digesters by *in situ* sampling, ultrafiltration, and gas chromatography with a flame ionization detector.

4.6. Feedstock loading limits in the microbial hydrolysis process (MHP)

At concentrations above 10% solids, dairy manure becomes too viscose to pump. Another limitation is the ratio of bicarbonate to cellulose in lignocellulose. Because bicarbonate is a product of methanogenesis in cow guts, bicarbonate is relatively high in dairy manure. For example, a full-grown cow releases about 200 L of methane daily and produces an equivalent amount of bicarbonate in the manure. Lignocellulose is a significant component of dairy manure, but the amount depends on the feed and breed of cow. The pH of raw dairy manure is controlled at about 7.8 by an ammonium bicarbonate buffer. In AD, bicarbonate is an inhibitor of both acetoclastic and syntrophic methanogenesis but must be maintained high enough to prevent acidification (souring) of the digester. The MHP requires bicarbonate as a reactant in pre-digestion to produce acetate in the ASB, and thus reduces the concentration of bicarbonate in the effluent going into the digesters and therefore reduces the required retention time. However, if

Please cite this article as: Hansen L.D. Thermodynamic method for analyzing and optimizing pretreatment/anaerobic digestion systems. Biofuel Research Journal 38 (2023) 1816-1829. DOI: 10.18331/BRJ2023.10.2.2

Table 13.
Digester effluents as a function of acetate concentration in the input and relative concentration of acetoclastic methanogens in the digester.

	Acetoclastic concentration	Effluent Acetate, mg L^{-1}	Biogas CH_4, L L^{-1} input	Biogas CO_2, L L^{-1} input	Biogas %CH_4	% VFA destruction	% alkalinity increase
Pre-digestion (MHP)	High	0	6.33	0.098	98.5	100	539
	Medium	5000	4.43	0.098	97.8	69	369
	Low	10000	2.54	0.098	96.3	38	200
	Zero	15000	0.64	0.098	86.7	7.1	31
No pre-digestion	High	0	2.54	0.098	96.3	100	200
	Medium	1667	1.90	0.098	95.1	73	144
	Low	3333	1.27	0.098	92.8	46	87
	Zero	5000	0.64	0.098	86.7	19	31

the mass ratio of bicarbonate to cellulose exceeds 1:1 in the feedstock, nearly all of the bicarbonate will be used up in the ASB, the pH drops to 5.3 or lower, and the digester will go sour because the carboxylate anions are protonated to carboxylic acids. The carboxylic acids are volatile and produce the horrible odors of a soured digester. Acetic acid smells like white vinegar; propionic acid smells like Swiss cheese; butyric and valeric acids smell like havarti cheese, rancid butter, and stinky feet, while caproic and higher carboxylic acids smell like goat cheese and a billy goat. Some people enjoy the odors and flavors in small doses, e.g., in cheeses, but in high doses and especially in mixtures, the barf potential is high. To avoid this, the ASB must not be fed too high a concentration of carbohydrates and cellulose.

4.7. Limitations and practical implications of the present study

A study of this kind requires developing a set of accurate, balanced equations for the specific chemical reactions in the process, which requires quantitative information on the proximate composition of the feedstock. See Figure 9 for a step-by-step process for doing this or a similar study.

Thus, the first limitation of this study is the lack of reliable proximate analysis of the composition of dairy manure. This study is also limited by the availability of reliable, standard Gibbs energies, $\Delta_f G°$, and the temperature dependence, for aqueous anions of VFAs for isomers of butyrate and valerate and VFAs with longer hydrocarbon chains than valerate. In fact, the $\Delta_f G°$ values for butyrate and valerate were estimates and not experimental values.

Note the blank slots left in Tables 6, 7, 8, and 10 in case these data become available. Unfortunately, to the best of the author`s knowledge, no laboratories are currently determining and publishing accurate $\Delta_f G°$ values for the other compounds and ions in potential feedstocks for AD. The VFA anions included in this study account for up to half the biogas produced, but the source of the rest is unknown organic compounds. On a practical note, this study shows why VFAs are useful indicators of the health of the consortium of microbes in a digester. The results lead to an understanding of the influence of feedstock composition on the optimum ratio of acetoclastic to syntrophic methanogenesis and the effect of that ratio on biogas composition. More information on the actual consortiums in working commercial digesters would help better future understanding.

5. Conclusions and future directions

Obtaining VS reduction as high as 75% with MHP requires a feedstock with less than 25% lignin and a mixed culture of acetoclastic methanogens, hydrogen-producing bacteria, and syntrophic methanogens. Under the conditions in the digester following MHP, acetoclastic methanogenesis is thermodynamically more favorable and kinetically faster than syntrophic methanogenesis. Because acetate is an inhibitor of syntrophic methanogenesis, the activity of acetoclastic methanogens must be high enough to maintain a very low acetate concentration to allow the maximum activity of syntrophic methanogens. Because syntrophic methanogenesis

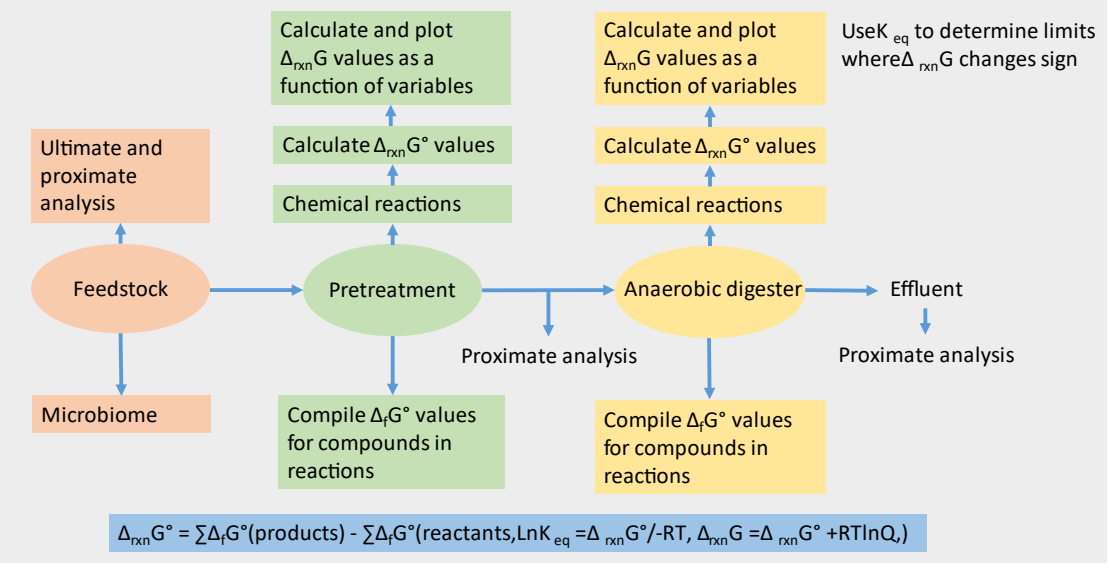

Fig. 9. Step-by-step procedure for the methodology used in this paper.

Please cite this article as: Hansen L.D. Thermodynamic method for analyzing and optimizing pretreatment/anaerobic digestion systems. Biofuel Research Journal 38 (2023) 1816-1829. DOI: 10.18331/BRJ2023.10.2.2

produces acetate catabolized by acetoclastic methanogens, if both types of methanogens are present in the AD seed, the culture in the digester should evolve to optimize the ratio of acetoclastic methanogens to syntrophic methanogens and maximize biogas production. This condition will be signaled by a constant, low acetate concentration in the AD and a relatively high and constant percent methane in the biogas. Judging from the results obtained in pilot plants, both acetoclastic and syntrophic methanogens may be present in manure from some dairies (Hansen et al., 2021). More information on the optimum growth temperatures of acetoclastic methanogens, hydrogen-producing bacteria, and syntrophic methanogens would help assess the relative merits of thermophilic and mesophilic digestion.

Because the model only provides relative rates, it can only be used to predict relative retention times in AD. Data on the kinetics of acetoclastic methanogenesis, hydrogen production by anaerobic bacteria, and syntrophic methanogenesis as functions of acetate, bicarbonate, and different VFA substrates would be useful for predicting optimum retention times. The available thermodynamic data are not sufficient to determine whether mesophilic or thermophilic digestion of the ASB effluent from dairy manure would give better results, and therefore data on the enthalpies of formation of aqueous anions of VFAs would be useful. But, in any case, the answer probably depends more on the species of methanogens available for seeding the digester. Mesophilic methanogens are much more common than thermophilic methanogens, and more data on the properties, growth conditions, and sources of acetoclastic methanogens would be helpful in seeding digesters.

Acknowledgements

The author thanks Dave Parry and Jaron Hansen for their helpful comments and the staff at the Harold B. Lee Library at BYU for their help accessing critical documents.

References

[1] Ahring, B.K., Sandberg, M., Angelidaki, I.J.AM., 1995. Volatile fatty acids as indicators of process imbalance in anaerobic digestors. Appl. Microbiol. Biotechnol. 43, 559-565.

[2] Baird, R.B., Eaton, A.D., Rice, E.W., Bridgewater, L. eds., 2017. Standard methods for the examination of water and wastewater, 23rd edition. American Public Health Association, Washington, D.C.

[3] Batstone, D.J., Keller, J., Angelidaki, I., Kalyuzhnyi, S.V., Pavlostathis, S.G., Rozzi, A., Sanders, W.T.M., Siegrist, H.A., Vavilin, V.A. 2002. The IWA anaerobic digestion model no 1 (ADM1). Water Sci. Technol. 45(10), 65-73.

[4] Batstone, D.J., Pind, P.F., Angelidaki, I., 2003. Kinetics of thermophilic, anaerobic oxidation of straight and branched chain butyrate and valerate. Biotech. Bioeng. 84(2), 195-204.

[5] Berghuis, B.A., Yua, F.B., Schulzc, F., Blainey, P.C., Woykec, T., Quake, S.R., 2019. Hydrogenotrophic methanogenesis in archaeal phylum Verstraetearchaeota reveals the shared ancestry of all methanogens. Proc. Natl. Acad. Sci. 116(11), 5037-5044.

[6] Bertacchi, S., Ruusunen, M., Sorsa, A., Sirviö, A., Branduardi, P., 2021. Mathematical analysis and update of ADM1 model for biomethane production by anaerobic digestion. Fermentation. 7(4), 237.

[7] Christensen, J.J., Hansen, L.D., Izatt, R.M., 1976. Handbook of proton ionization heats and related thermodynamic quantities. John Wiley and Sons, New York.

[8] Conrad, R., 1999. Contribution of hydrogen to methane production and control of hydrogen concentrations in methanogenic soils and sediments. FEMS Microbiol. Ecol. 28(3), 193-202.

[9] Conrad, R., 2020. Importance of hydrogenotrophic, aceticlastic and methylotrophic methanogenesis for methane production in terrestrial, aquatic and other anoxic environments: a mini review. Pedosphere. 30(1), 25-39.

[10] Denbigh, K.G., 1951. The Thermodynamics of the Steady State. John Wiley and Sons, New York.

[11] Goldberg, R.N., Kishore, N., Lennen, R.M., 2002. Thermodynamic quantities for the ionization reactions of buffers. J. Phys. Chem. Ref. Data. 31(2), 231-370.

[12] Gupta, K.K., Aneja, K.R., Rana, D., 2016. Current status of cow dung as a bioresource for sustainable development. Bioresour. Bioprocess. 3, 28.

[13] Hansen, J.C., Aanderud, Z.T., Reid, L.E., Bateman, C., Hansen, C.L., Rogers, L.S., Hansen, L.D., 2021. Enhancing waste degradation and biogas production by pre-digestion with a hyperthermophilic anaerobic bacterium. Biofuel Res. J. 31, 1433-1443.

[14] Holtzapple, M.T., Wu, H., Weimer, P.J., Dalke, R., Granda, C.B., Mai, J., Urgun-Demirtas, M., 2022. Microbial communities for valorizing biomass using the carboxylate platform to produce volatile fatty acids: a review. Bioresour. Technol., 344, 126253.

[15] Kataeva, I., Foston, M.B., Yang, S.J., Pattathil, S., Biswal, A.K., Poole II, F.L., Basen, M., Rhaesa, A.M., Thomas, T.P., Azadi, P., Olman, V., Saffold, T.D., Mohler, K.E., Lewis, D.L., Doeppke, C., Zeng, Y., Tschaplinski, T.J., York, W.S., Davis, M., Mohnen, D., Xu, Y., Ragauskas, A.J., Ding, S.Y., Kelly, R.M., Hahn M.G., Adams, M.W.W., 2013. Carbohydrate and lignin are simultaneously solubilized from unpretreated switchgrass by microbial action at high temperature. Energy Environ. Sci. 6(7), 2186-2195.

[16] Kato, S., Watanabe, K., 2010. Ecological and evolutionary interactions in syntrophic methanogenic consortia. Microbes Environ. 25(3), 145-151.

[17] Kato, S., Yoshida, R., Yamaguchi, T., Sato, T., Yumoto, I., Kamagata, Y., 2014. The effects of elevated CO_2 concentration on competitive interaction between aceticlastic and syntrophic methanogenesis in a model microbial consortium. Front. Microbiol. Systems Microbiol. 5, 575.

[18] Lyu Z., Shao N., Akinyemi T., Whitman W.B., 2018. Methanogenesis. Curr. Biol. 28(13), R727-R732.

[19] Mackie, R.I., White, B.A., Bryant, M.P., 1991. Lipid metabolism in anaerobic ecosystems. Crit. Rev. Microbiol. 17(6), 449-479.

[20] Miller, S.L., Smith-Magowan, D., 1990. The Thermodynamics of the Krebs Cycle and Related Compounds. J. Phys. Chem. Ref. Data. 19(4), 1049-1073.

[21] Millero, F.J., Pierrota, D., Lee, K., Wanninkhof, R., Feely, R., Sabine, C.L., Key, R.M., Takahashi, T., 2002. Dissociation constants for carbonic acid determined from field measurements. Deep Sea Res. Part I. 49(10), 1705-1723.

[22] Nikafshar, S., Zabihi, O., Hamidi, S., Moradi, Y., Barzegar, S., Ahmadi, M., Naebe, M., 2017. A renewable bio-based epoxy resin with improved mechanical performance that can compete with DGEBA. RSC Adv. 7(14), 8694-8701.

[23] Pind, P.F., Angelidaki, I., Ahring, B.K., 2003a. Dynamics of the anaerobic process: effects of volatile fatty acids. Biotechnol. Bioeng. 82(7), 791-801.

[24] Pind, P.F., Angelidaki, I., Ahring, B.K., 2003b. A new VFA sensor technique for anaerobic reactor systems. Biotechnol. Bioeng. 82(1), 54-61.

[25] Popovic, M., Woodfield, B.F., Hansen, L.D., 2019. Thermodynamics of hydrolysis of cellulose to glucose from 0 to 100°C: cellulosic biofuel applications and climate change implications. J. Chem. Thermo. 128, 244-250.

[26] Qian, H., Chen, W., Zhu, W., Liu, C., Lu, X., Guo, X., Huang, D., Liang, X., Kontogeorgis, G.M., 2019. Simulation and evaluation of utilization pathways of biomasses based on thermodynamic data prediction. Energy. 173, 610-625.

[27] Rehman, M.L.U., Iqbal, A., Chang, C.C., Li, W., Ju, M., 2019. Anaerobic digestion. Water Environ. Res. 91, 1253-1271.

[28] Schink, B., 1997. Energetics of syntrophic cooperation in methanogenic degradation. Microbiol. Molecular Biol. Rev. 61(2), 262-280.

[29] Sinbuathong, N., Sillapacharoenkul, B., Palakas, S., Kahraman, U., Dincer, I., 2022. Using sugarcane leaves and tops for exploiting higher methane yields: an assessment study. Int. J. Hydrog. Energy. 47(77), 32861-32875.

Please cite this article as: Hansen L.D. Thermodynamic method for analyzing and optimizing pretreatment/anaerobic digestion systems. Biofuel Research Journal 38 (2023) 1816-1829. DOI: 10.18331/BRJ2023.10.2.2

[30] Skorek-Osikowska, A., 2022. Thermodynamic and environmental study on synthetic natural gas production in power to gas approaches involving biomass gasification and anaerobic digestion. Int. J. Hydrogen Energy. 47(5), 3284-3293.
[31] Thauer, R.K., Jungermann, K., Decker, K., 1977. Energy conservation in chemotrophic anaerobic bacteria. Bacteriol. Rev. 41(1), 100-180.
[32] Vanwonterghem, I., Evans, P.N., Parks, D.H., Jensen, P.D., Woodcroft, B.J., Hugenholtz, P., Tyson, G.W., 2016. Methylotrophic methanogenesis discovered in the archaeal phylum Verstraetearchaeota. Nature Microbiol. 1, 16170.
[33] Wagman, D.D., Evans, W.H., Parker, V.B., Schumm, R.H., Halow, I., Bailey, S.M., Churney, K.L., Nuttall, R.L., 1982. The NBS tables of chemical thermodynamic properties. selected values for inorganic and C_1 and C_2 organic substances in SI units. J. Phys. Chem. Ref. Data. 18(4), 1807-1812.
[34] Westerholm, M., Calusinska, M., Dolfing, J., 2022. Syntrophic propionate-oxidizing bacteria in methanogenic systems FEMS Microbiol. Rev. fuab057, 46(2), fuab057.

Prof. Lee D. Hansen is Prof. Emeritus in the Department of Chemistry and Biochemistry at the Brigham Young University, Provo, UT. During his career, he has published over 300 papers in peer-reviewed journals on a wide range of topics. His specialties are calorimetry, thermodynamics, and the kinetics and energetics of biological systems.

Please cite this article as: Hansen L.D. Thermodynamic method for analyzing and optimizing pretreatment/anaerobic digestion systems. Biofuel Research Journal 38 (2023) 1816-1829. DOI: 10.18331/BRJ2023.10.2.2